

**Illuminating snow droughts: The future of Western  
United States snowpack in the SPEAR large ensemble**

**Julian Schmitt<sup>1</sup>, Kai-Chih Tseng<sup>234</sup>, Mimi Hughes<sup>5</sup>, Nathaniel Johnson<sup>2</sup>**

<sup>1</sup>Harvard University

<sup>2</sup>Geophysical Fluid Dynamics Laboratory

<sup>3</sup>Princeton University

<sup>4</sup>Department of Atmospheric Sciences, National Taiwan University, 10617, Taipei, Taiwan

<sup>5</sup>Earth System Research Laboratories/ Physical Sciences Laboratory

**Key Points:**

- Driven largely by the last two decades, western U.S. severe snow droughts have increased in frequency by 40-50% across all major watersheds over the last 60 years.
- The SPEAR climate model accurately simulates the rapid acceleration of western U.S. severe snow drought occurrence that began in the early 2000s.
- SPEAR projects that increasing temperatures will cause the West to transition to a no-snow environment by the end of the 21st century.

16      **Abstract**

17      Seasonal snowpack in the Western United States (WUS) is crucial for meeting summer  
 18      hydrological demands, reducing the intensity and frequency of wildfires, and supporting  
 19      snow-tourism economies. While the frequency and severity of snow drought is ex-  
 20      pected to increase under continued global warming, quantifying both the response of snow  
 21      drought to radiative forcing and uncertainties owing to internal climate variability pro-  
 22      vides a significant challenge. To evaluate the projected changes in WUS snow droughts  
 23      and the uncertainties tied to internal climate variability, we analyzed a 30-member large  
 24      ensemble of a global climate model with moderately high atmospheric resolution ( $\sim 50\text{km}$ ),  
 25      the Seamless System for Prediction and EArth System Research (SPEAR). To monitor  
 26      changes in WUS snow droughts in both observations and SPEAR, we developed a non-  
 27      parametric drought classification scheme for monthly snowpack. We find that SPEAR  
 28      projects dramatic increases in snow droughts, with a 8.8-fold increase in snow drought  
 29      occurrence under SSP5-8.5 and a 5.2-fold increase under SSP2-4.5 emissions pathways  
 30      by 2100 averaged over the ensemble. We found these changes to be primarily driven by  
 31      an increase in average monthly temperature anomalies. We define no-snow conditions  
 32      as when over 90% of a watershed's historically snowy region's April snowpack is less than  
 33      10% of the historical April snowpack average. When tracking the transition to no-snow  
 34      conditions, we found large variability in onset times attributable to internal climate vari-  
 35      ability. Across the SSP5-8.5 30-member ensemble spread, SPEAR projects that Califor-  
 36      nia, for example, could experience no-snow conditions as early as 2058 or as late as 2096.  
 37      This wide range emphasizes the large irreducible uncertainty of internal climate variabil-  
 38      ity on WUS snow drought changes that has large implications for water management and  
 39      habitability over the coming century.

40      **Plain Language Summary**

41      When winter snow on the ground is significantly less than normal, a region is said  
 42      to experience a snow drought. Recently, the Western United States has seen a sharp uptick  
 43      in the frequency of severe snow droughts. Since the region depends on stored mountain  
 44      snowpack, the snow droughts have amplified water shortages and wildfires. Here, we use  
 45      a new climate model to examine trends in snow droughts through 2100, finding that un-  
 46      der a high emission scenario, they could increase nearly 9 fold in frequency by 2100. Us-  
 47      ing a large ensemble model, we examine how internal climate variability impacts how  
 48      quickly regions reach a state of "no-snow" in April. California, for example, reaches no-  
 49      snow conditions anywhere from 2058 to 2096 under the high emissions scenario.

50      **1 Introduction**

51      Mountains in the Western United States (WUS) have been coined the "water tow-  
 52      ers" of the West, storing winter precipitation as snow and releasing it during the dry spring  
 53      and summer as meltwater to populations which have high, and ever-increasing water needs  
 54      (Barnett et al., 2005). Alongside direct benefits of sustained snowpack to human irri-  
 55      gation and water needs, several indirect benefits such as reduced forest fires (Trujillo et  
 56      al., 2012; Gergel et al., 2017) and improved snow tourism economics, makes snowpack  
 57      essential to the WUS' environment and its people. Low or variable snowpack means the  
 58      opposite: decreased water security, increased fire season activity, and unpredictable snow  
 59      conditions for tourism (Wobus et al., 2017). Despite large variability from season to sea-  
 60      son, climate change is already having a measurably significant impact on WUS snow-  
 61      pack, moving towards decreasing snowpack, particularly in late winter (Barnett et al.,  
 62      2005; Huning & AghaKouchak, 2020). When snowpack, or snow-water equivalent (SWE  
 63      - the depth of water if all snow melted instantaneously) levels fall significantly below nor-  
 64      mal, the region is said to experience a snow drought. Snow drought affects the WUS'

65 economy and human activities, even areas which are not necessarily covered in winter  
66 snowpack that instead rely on streamflow for crop production or human consumption.

67 While hydrological drought has immediate impacts on water resources and availability,  
68 the impact of snow droughts (SDs) is typically not felt until summer when early  
69 or low snowmelt can exacerbate meteorological drought. Mountains also play a key role  
70 in the WUS water supply, as their lower temperatures and higher precipitation capture  
71 significant reserves in snow pack. The WUS dry summers makes it reliant on a steady  
72 supply of melting water throughout much of the summer and winters with low snowpack  
73 typically exacerbating water shortages and wild fires (Barnett et al., 2005; Trujillo et al.,  
74 2012; Gergel et al., 2017). The type of snow drought also has significant impact on the  
75 effects. Dry snow droughts occur when a lack of precipitation results in low stream flow  
76 during the melt season, while a warm snow drought is characterized by rapid early sea-  
77 son snowmelt resulting in increased reservoir flood risk in early spring, followed by drought  
78 conditions as mountain snow is quickly depleted (Harpold et al., 2017). Shrestha et al.  
79 (2021) have shown that there is a critical threshold of -6 to -5°C for average winter tem-  
80 peratures above which additional warming begins to significantly decrease snowpack. The  
81 WUS falls into this category and therefore its snowpack is vulnerable to any level of warm-  
82 ing (Shrestha et al., 2021).

83 Previous literature has shown that there remains large observational uncertainty  
84 in climatological SWE across the WUS, primarily due to low sampling and trouble re-  
85 solving mountain snowpack, particularly in regions with complex terrain due to addi-  
86 tional uncertainty in temperature and precipitation. Coupled global climate models (GCMs)  
87 face similar challenges but to a greater degree because they simulate, not observe, tem-  
88 perature and precipitation, and are without access to the high-resolution of a variable  
89 infiltration capacity (VIC) model essential over complex terrain (McCrary et al., 2017;  
90 Kim et al., 2021; Wrzesien et al., 2019; McCrary et al., 2022). Despite large biases and  
91 variability in simulating climatological SWE, these models exhibit more uniformity in  
92 simulating robust decreases in WUS SWE (Matiu & Hanzer, 2022). Huning and AghaK-  
93 ouchak (2020) have also shown that SD total duration, average duration, and intensity  
94 in the WUS has increased by 28% between 1980 and 2018, while Shrestha et al. (2021)  
95 finds that conditions are expected to continue to worsen because of the WUS' low lat-  
96 itude.

97 To investigate historical and future changes in SD frequency and intensity we use  
98 a 30-member initial condition state-of-the-art coupled large ensemble global climate model,  
99 called the Seamless System for Prediction and EArth System Research Large Ensem-  
100 ble (hereafter SPEAR). We first show that SPEAR simulations of WUS severe snow drought  
101 (D2+ SD) changes across the historical period (1921-2011) are consistent with those in  
102 an observational dataset and with previous studies (Livneh et al., 2013; Huning & AghaK-  
103 ouchak, 2020). Here, the D2+ SD classification includes all snow droughts in the D2, D3,  
104 and D4 categories. We then explore the magnitude of the projected changes by assess-  
105 ing the proportion of months that experience D2+ SD, looking both at the ensemble mean  
106 spatio-temporally alongside the ensemble spread through time. To further investigate  
107 what is driving the rapid acceleration in D2+ SD frequency, we decompose drought con-  
108 ditions by temperature and precipitation deviation to assess how the conditions under  
109 which snow droughts occur changes through time. We then provide a watershed-level  
110 assessment of the risk of becoming “snow-free” by the end of the century that explicitly  
111 accounts for both scenario uncertainty and internal climate variability.

112 By quantifying the uncertainty of these trends that is attributable to both inter-  
113 nal climate variability and emissions uncertainty, we assess the distribution of D2+ SD  
114 frequency outcomes, the variability in average drought/non-drought conditions, and the  
115 distribution of the timing to a no-snow regime by WUS watershed region. We look to  
116 both verify the SPEAR ensemble simulations by looking over the historical period (1921-  
117 2014) with observed time-varying natural and anthropogenic radiative forcing, and to

118 examine future projections (2014-2100) under a “middle of the road” (SSP2-4.5) and a  
 119 high emissions scenario (SSP5-8.5) (Delworth et al., 2020). The 30 ensemble runs for each  
 120 future scenario and two concentration pathways allow us to explore variability across not  
 121 only the emissions scenarios but also within the ensemble under identical emissions to  
 122 estimate the internal climate variability.

## 123 2 Data and Methods

### 124 2.1 SPEAR Large Ensemble Global Climate Model

125 To assess historical and future changes in snow drought, we analyzed snow water  
 126 equivalent (SWE) values across the Western United States from the 30-member **S**eamless  
 127 **P**eriodic **E**nsemble **R**esearch (hereafter SPEAR)  
 128 (Delworth et al., 2020). SPEAR is a coupled global climate model recently developed  
 129 at the NOAA Geophysical Fluid Dynamics Laboratory (GFDL) that is designed for im-  
 130 proved prediction on seasonal to decadal timescales. SPEAR comprises GFDL’s AM4  
 131 atmosphere, LM4 land, MOM6 ocean, and SIS2 sea-ice models. These component mod-  
 132 els are the same as GFDL’s Global Climate Model version 4 (CM4, Held19), which is  
 133 a contributor to the Coupled Model Intercomparison Project, phase 6 (CMIP6), but SPEAR’s  
 134 configuration and physical parameterization choices are optimized for climate prediction  
 135 and projection from seasonal to centennial timescales. SPEAR has moderately high res-  
 136 olution in the atmosphere and land (50 km resolution) and a coarser ocean and sea ice  
 137 horizontal resolution of about 1° which telescopes to 0.33° meridional spacing near the  
 138 equator.

139 We specifically use SPEAR’s monthly SWE, temperature, and precipitation across  
 140 the historical period, from 1921-2014, as well as projections from 2014-2100 under SSP2-  
 141 4.5 and SSP5-8.5 emissions scenarios.

### 142 2.2 Observational Data

143 To evaluate SPEAR’s historical simulation of SWE, temperature, and precipita-  
 144 tion we use an observations-based dataset (Livneh et al., 2013), available from 1915 to  
 145 2011, hereafter the Livneh dataset. Livneh is statistically gridded from in situ observa-  
 146 tions of precipitation and temperature to 1/16° resolution, and contains daily temper-  
 147 ature, precipitation observations, plus SWE estimates which are generated using the VIC  
 148 land model. To compare with the SPEAR ensemble members, we re-gridded Livneh to  
 149 SPEAR’s 1/2° grid and re-sampled to SPEAR’s monthly timescale. Despite incorpor-  
 150 ating observational data, SWE has perennially been hard to constrain (Wrzesien et al., 2019).  
 151 Many recent papers have found SWE estimates to vary widely, upwards of a factor of  
 152 3 in some cases (Wrzesien et al., 2019) leading us to expect significant absolute biases  
 153 between SWE estimates (McCrary et al., 2017, 2022), of which Livneh is only one rep-  
 154 resentation. To overcome this issue, we focus our analysis on proportional changes, com-  
 155 paring SWE values to their own historical distributions within each dataset, and then  
 156 comparing these relative changes across datasets.

157 We chose 1921-2011 as our historical period as it is the overlapping period between  
 158 the Livneh dataset and the historical SPEAR dataset. This provided 90 complete win-  
 159 ters (91 years) which we used to validate SPEAR and to develop a baseline to which we  
 160 compare the modeled future climatology. We chose to consider data at monthly resolu-  
 161 tion intervals for three reasons: (1) data availability, as SPEAR only recorded SWE at  
 162 monthly intervals, (2) consistency with previous studies, as other papers have done sim-  
 163 ilar analysis (Huning & AghaKouchak, 2020), and (3) monthly resolution is an appro-  
 164 priate timescale for monitoring snow drought.

165        **2.3 Comparison of a Climate Ensemble to Observations**

166        A previous study in Maher et al. (2022) assesses Pacific Decadal Oscillation (PDO)  
 167        teleconnections to temperature and precipitation patterns across North America by val-  
 168        idating observational data against 5 large ensembles, including SPEAR. They find that  
 169        SPEAR has both low bias in representing PDO, particularly along the US West Coast.  
 170        In addition to the assessment in Delworth et al. (2020), finding minimal temperature and  
 171        a slight precipitation biases, this study further validates SPEAR as accurately reproduc-  
 172        ing atmospheric conditions across WUS. Given these two studies have shown SPEAR  
 173        to well-represent atmospheric conditions across the WUS, we focused our validation of  
 174        SPEAR on WUS SWE, in addition to brief comparisons of precipitation and temper-  
 175        ature of our observational Livneh dataset. We first compare the historical SPEAR runs  
 176        to the Livneh dataset over the historical period. As Livneh contains a single realization  
 177        of the historical period, e.g. what actually happened, while the SPEAR ensemble runs  
 178        capture many possible historical climates, we do not expect the Livneh measurement to  
 179        align with the SPEAR ensemble mean because changes to the ensemble mean represent  
 180        the radiatively forced component of the climate with internal variability filtered out. The  
 181        internal variability is an essential component of individual realizations, contributing sig-  
 182        nificantly to inter-model spread in CMIP multi-model ensembles (Deser et al., 2020) and  
 183        is essential for modeling extremes. We do expect, however, that SPEAR will simulate  
 184        a realization of the climate at least as extreme as the observed historical climate over  
 185        most regions, although with only 30 members it's still reasonable to expect some obser-  
 186        vations may fall outside of the SPEAR spread. Thus, if a metric of change, e.g. change  
 187        in snow drought frequency, derived from the Livneh dataset falls within the ensemble  
 188        spread of the same metric in the SPEAR ensemble across many subregions, we can as-  
 189        sume SPEAR produces a realistic historical climate.

190        **2.4 Drought Classification**

191        Before we can begin to assess changes in snow drought measurements, we must first  
 192        define snow drought, which is based on the historical distribution of SWE values per month  
 193        by both grid-cell and region. For subsequent analysis, we restrict our region of study to  
 194        areas that historically have seasonal snowpack maxima that average above 20mm SWE,  
 195        based on the SPEAR ensemble mean, we call this the “historically snowy” region. This  
 196        ensures regions that do not typically have snow are not eligible for classification as snow  
 197        drought.

198        Our methodology uses standardized indices which compare a region’s SWE values  
 199        to its historical climatology, using the US Drought Monitor’s drought classification method  
 200        for hydrological drought to categorize observations into descriptive bins; near normal,  
 201        abnormally dry, and moderate, severe, extreme, and exceptional drought, see Figure S1  
 202        (Svoboda et al., 2002). Here we use a non-parametric empirical model for SWE, tem-  
 203        perature, and precipitation deviations. Without assuming the underlying distributions,  
 204        a non-parametric model allows us to efficiently capture the variability without impos-  
 205        ing subjective constraints on the data and allows us to compare drought frequency and  
 206        severity across different hydrological regions and different datasets.

207        We assign each winter month of the year (Oct-April) a score based on the histor-  
 208        ical conditions at that location. Our time indices are by year and month, e.g.  $t_{1931,1}$  for  
 209        January 1931, and spatial indices are at intervals of 0.5 degrees of latitude and longitude.  
 210        Thus  $s_{i,j}^{t_{1931,1}}$  corresponds to a SWE value at latitude-longitude pair  $(i, j)$  during January  
 211        1931. We now compute an empirical distribution over  $\mathbf{S}_{i,j}^k = (s_{i,j}^{t_{1921,k}}, s_{i,j}^{t_{1922,k}}, \dots, s_{i,j}^{t_{2011,k}})$ ,  
 212        representing the SWE values during month  $k$  at location  $(i, j)$  over the historical period.  
 213        We assign z-scores to each location and time stamp using the empirical cumulative dis-  
 214        tribution function,  $\hat{F}_{i,j}^k$  which assigns each SWE value a number in  $(0, 1)$  based on the  
 215        proportion of the observed data in  $\mathbf{S}_{i,j}^k$  that fall below it. In equation 1,  $\mathbb{I}$  represents an  
 216        element-wise indicator for each element of  $\mathbf{S}_{i,j}^k$  being below  $x$  and  $N$  represents the to-

tal number of measurements, in this case  $2011 - 1921 = 90$ .

$$\hat{F}_{i,j}^k(x) = \frac{\text{no. of SWE values less than } x}{N_m} = \frac{1}{N_m} \sum_{l=1}^{N_m} \mathbb{I}(S_{i,j}^k < x) \quad (1)$$

For each observed or simulated SWE value,  $s_{i,j}^{t_{y,k}}$ , we can then compute the z-score by inserting the SWE value into the corresponding  $\hat{F}$  and then into the inverse normal distribution. We refer to these scores as ZSWE, which are indexed by location, month, and year, and define them as such:

$$ZSWE_{i,j}^{y,m} = \Phi\left(\hat{F}_{i,j}^m(s_{i,j}^{y,m})\right) \quad (2)$$

We classify each month by a drought severity label D0-D4, with NN classifying a month as near normal and W0-W4 increasingly wet months see Table S1 for the full classification scheme. While we mostly use this framework to classify snow droughts, we extend the methodology to temperature and precipitation classification as needed. A similar empirically derived methodology is used by Huning and AghaKouchak (2020) to classify snow droughts across the Alps, Himalayas, and Western United States. More generally, this framework is inspired by the US Drought Monitor which uses the same D0-D4 classification. Their classification scheme, however, is not purely statistical, instead relying on local experts for the final say on the drought classification. As we cannot rely on experts, our model attempts to match the frequency of meteorological droughts in the US Drought Monitor with snow drought frequency. While our method may result in a mismatch of SWE values and impact in some locations, it provides a statistical way to quickly capture extremes without gathering detailed human and environmental data for each pixel.

## 2.5 Computing Changes in Snow Drought

We can now apply our drought classification scheme to calculate changes in snow drought across the historical period. We used two 41-year windows containing 40 complete winters, with our early historical period ranging from 1930-1970 and our late historical period from 1971-2011. We aggregate snowpack by HUC2 region, see Figure 1c, and count the total number of occurrences of each extreme event, where we define an extreme event as that which meets a D2+ classification or a z-score of  $< -1.3$ , e.g.  $\mathbb{I}(Z_R^t < -1.3)$  for region  $R$  at time  $t$ . The percent change for a given region,  $\Delta_R$ , is derived via

$$\Delta_R = \frac{\sum_{t'} \mathbb{I}(Z_R^{t'} < -1.3)}{\sum_t \mathbb{I}(Z_R^t < -1.3)} \quad \text{for } t \in (1930, 1970), t' \in (1971, 2011) \quad (3)$$

For example, the Livneh dataset experienced 27 months of D2+ SD in the early historical period for the Upper Colorado Region, with 28 observations in the late historical period, translating to an increase of 3.7%. We leverage the ensemble spread below to determine whether the overall trend is significant.

## 2.6 Snow Transition Threshold

We are also motivated to determine how a changing snowpack will affect water resources more directly than looking at droughts alone. Broadly we want to determine when a shifting climate will begin to severely and persistently impact snow as a water resource. Long-term droughts are particularly damaging, as one or two years of low snow-pack can be buffered by groundwater, above-ground reservoirs, or stored in live biomass. Thus, we are particularly interested in determining when no-snowpack is expected to become systemic (Siirila-Woodburn et al., 2021).

Alongside changes in snow drought characteristics, understanding the fraction of snow that remains in a typical year is important for water management (Harpold et al.,

2017). To assess this threat, we calculate the fraction of April SWE that remains in historically snowy regions across each of the 5 HUC2 watersheds. We classify an April ( $m = 4$ ) grid cell  $s_{i,j}^{t,4}$  as no-snow (or snow free) for that year if there is *at most* 10% of the historical snowfall average remaining at the location (Siirila-Woodburn et al., 2021). We then calculate the regional no-snow area proportion as the fraction of the historically snowy region which experiences those conditions. We let  $\mathcal{N}_R^Y$  to denote this no-snow area proportion, where  $R$  represents the region, and  $Y$  the year. As before,  $t_Y \bar{S}_{i,j}^{t_Y,4}$  is the average historical SWE value for the grid cell and  $s_{i,j}^{t_Y,4}$  the SWE value for the specific year. Using 10% as our snow free threshold,  $\mathcal{T} = 0.1$ , then  $\mathcal{N}_R^Y$  can be written as:

$$\mathcal{N}_R^Y = \frac{\sum_{(i,j) \in R} \mathbb{I}(s_{i,j}^{t_Y,4} < \mathcal{T} \cdot \bar{S}_{i,j}^{t_Y,4})}{|(i,j) \in R|}. \quad (4)$$

Thus we have a fraction of the historically snowy region that is snow free in a given year in April. To assess when no-snow conditions become endemic, we apply a 10 year moving-window mean and then define the no-snow transition time as the year when the moving-window mean *last* crosses the area threshold,  $\mathcal{A} = 0.5, 0.75, 0.9$  before 2100. Applying this procedure to all ensemble members, we compute a distribution for when these conditions are likely to become endemic. Formally, the no-snow transition time,  $\mathcal{T}$ , is given by:

$$\mathcal{T} := \left[ \min t : \mathcal{N}_R^{t'} \geq \mathcal{A} \forall t < t' \leq 2100 \right]. \quad (5)$$

Where  $\tilde{\mathcal{N}}_R^{t'}$  gives the moving-window mean fraction of region  $R$  that experiences no-snow conditions at time  $t'$ . By requiring the moving-window average to be above  $\mathcal{A}$  for all subsequent years (until 2100),  $\mathcal{T}$  is uniquely determined. For a graphical explanation of this method, please refer to Figure S4.

### 3 Results

#### 3.1 SPEAR Model Evaluation

##### 3.1.1 SPEAR Ensemble Mean Bias

We begin our evaluation with a brief comparison of Livneh and SPEAR winter mean SWE and precipitation. We do this by averaging over the winter season, Oct-April, for the period of dataset overlap, 1921-2011. We find that SPEAR has a negative snow bias across much of the Mountain West, see Figure 1. In particular, regions characterized by high elevation often have SWE values over 100% higher in the Livneh dataset than SPEAR. This is not particularly surprising however, as resampling the 1/16° Livneh grid to the 1/2° grid for comparison with the coarse SPEAR data introduces bias as higher elevations have disproportionately more snow as compared with elevation (McCrary et al., 2022). Precipitation biases are consistently high across much of the Western US as seen in Figure 1 – these findings are consistent with Delworth et al. (2020).

However, despite these large absolute biases, we can still use SPEAR to quantify future snow droughts if it reasonably reproduces trends in SWE, temperature, and precipitation. To make these comparisons we leverage the distribution of the SPEAR large ensemble, allowing us to create a distribution of potential historical outcomes, to compare against the Livneh dataset.

##### 3.1.2 Evaluating Snow Drought Changes across the Historical Period

When examining historical changes, we find that SPEAR historical snow drought and temperature trends are already significant, based on a 95% confidence interval for the ensemble mean assuming an underlying normal distribution in changes. Changes in SWE across all 5 studied HUC2 regions, the Upper Colorado, Lower Colorado, Great Basin, Pacific Northwest, and California regions (abbreviated UC, LC, GB, PNW, and

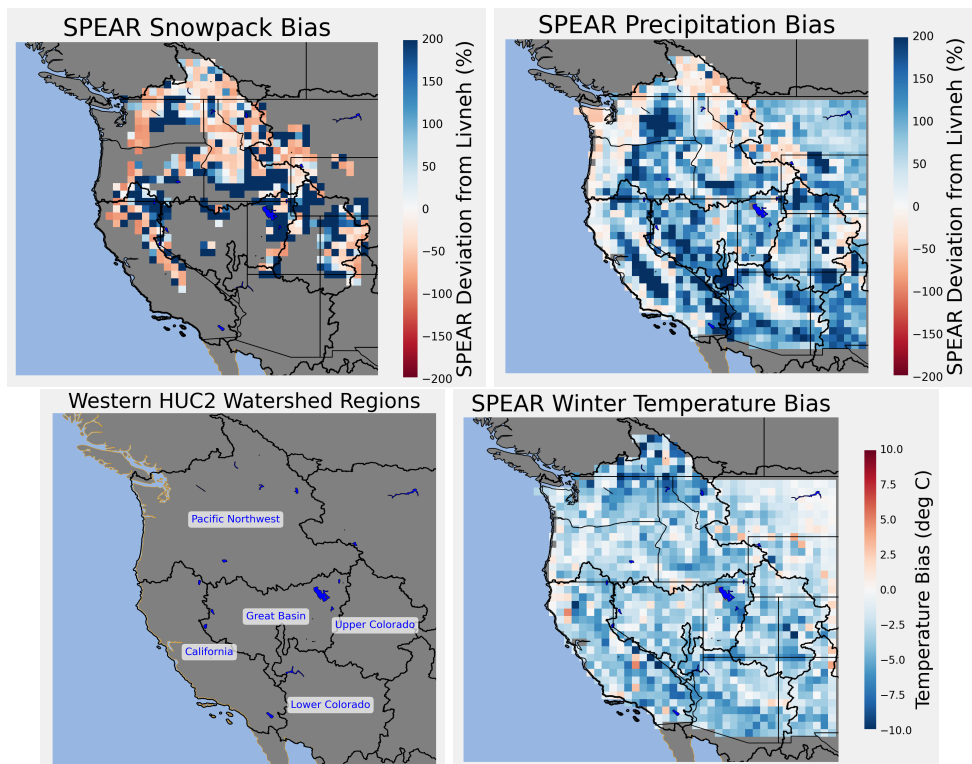


**Figure 1.** Clockwise from top left: SPEAR winter (Oct-Apr) (a) snowpack (%), (b) winter precipitation (%) and winter temperature biases as compared to Livneh. (d) depicts the 5 study HUC2 regions of interest.

<b>Historical Changes in Snow Drought Frequency by Region (%)</b>					
HUC2 Region	Livneh Increase	SPEAR Avg Increase	SPEAR Mean	95% CI	SPEAR Ensemble Range
Upper Colorado	4	53	[30, 77]	[-50, 236]	
Lower Colorado	14	26	[13, 40]	[-39, 107]	
Great Basin	45	48	[26, 70]	[-40, 225]	
Pacific Northwest	-55	43	[16, 71]	[-68, 255]	
California	9	46	[25, 67]	[-34, 192]	

**Figure 2.** Summary table of Livneh and SPEAR average D2+ SD frequency changes for each of the 5 Western HUC2 regions. Changes are measured between the early (1930-1970) and late (1971-2011) historical periods. As SPEAR is a large ensemble we include a 95% confidence interval which assumes normally distributed changes, and a range of changes across the ensemble.

CA) show with ensemble means ranging from 26% (LC) to 53% (UC) increases in D2+ SD occurrence, as in Table 2. The Livneh dataset always falls within the ensemble spread (Table 2), although it is not always in the ensemble mean 95% CI. We present the distribution of D2+ SDs across the historical period (1980-2011) for SPEAR ensemble members, the SPEAR mean, and confidence interval, along with the Livneh observation in Figure 3. These results were consistent with findings in Huning and AghaKouchak (2020), who use 1980-2018 as their historical period — in fact, the 95% confidence interval for the SPEAR ensemble mean across 4 of the 5 regions contains the 28% benchmark for drought intensity increases found in Huning and AghaKouchak (2020), with only the UC interval exceeding the benchmark with a 30% lower bound on historical D2+ SD increases. While we were unable to use an identical historical period due to data constraints, the agreement helps to further validate the SPEAR ensemble. See supplemental Text S1 and Figure S2 for an analysis of changes in precipitation and temperature across the historical period.

### 3.2 Analyzing Snowpack into the 21<sup>st</sup> Century: Accelerating Loss

We next shift our attention to projected changes in 21<sup>st</sup> century D2+ SD, focusing first on changes in droughts classified directly with our ZSWE metric. We construct our empirical CDF  $\hat{F}_{i,j}^k$  distributions from the historical period (1921-2011) and calculate corresponding ZSWE scores for each winter month across the historically snowy west 2014-2100 for all 30 ensemble members. Projected changes in snowpack are dramatic, with rapid increases in D2+ SD occurring at mid-century (Figure 4). Under SSP5-8.5 we find that towards the end of the century, all regions are projected to experience severe drought, or more severe, during most months. Under SSP2-4.5, changes in snow drought occurrence at the end of the century resemble snow drought conditions near mid-century in the SSP5-8.5 ensemble. Thus, a higher forcing scenario is expected to accelerate SWE decreases by several decades by the end of the century. Snow drought percentages for all 18 study decades are shown in Figure S3.

Examining the distribution of D2+ SDs spatially in Figure 4, a pattern of regional “hot-spots” emerge, where D2+ SD frequency is consistently higher in certain regions beginning in 2030. For example the Washington Cascades and Colorado Rockies are predicted to experience more frequent snow drought occurrences across all decades than regions in south-central Idaho and the California Sierra Nevada. We expected to see the more southern basins have more dramatic increases in snow drought, such as the Colorado Rockies or California regions, as even low amounts of warming at southern lat-

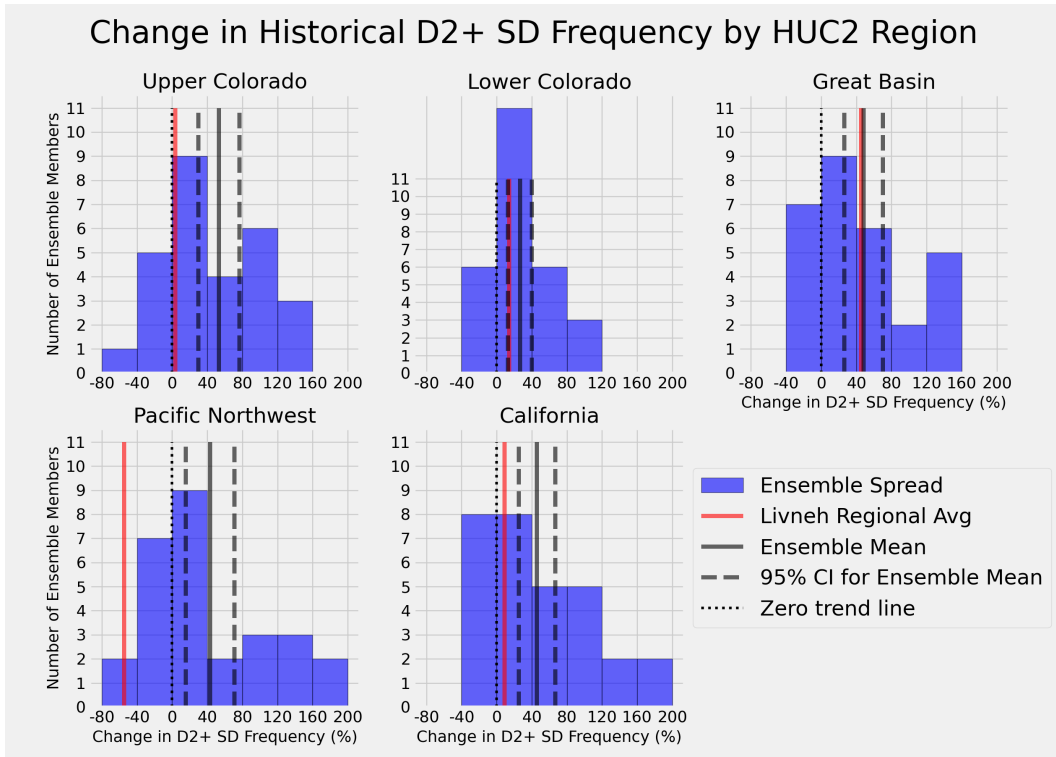


**Figure 3.** Comparison of SPEAR estimated D2+ SD increases across the historical to Livneh observed increases. The SPEAR distribution is given by the histogram in blue, with the red vertical line representing the observed change in the Livneh dataset. The solid and dashed gray lines represent the mean and 95% confidence interval for each region's ensemble mean, while the dotted line represents the zero trend line.

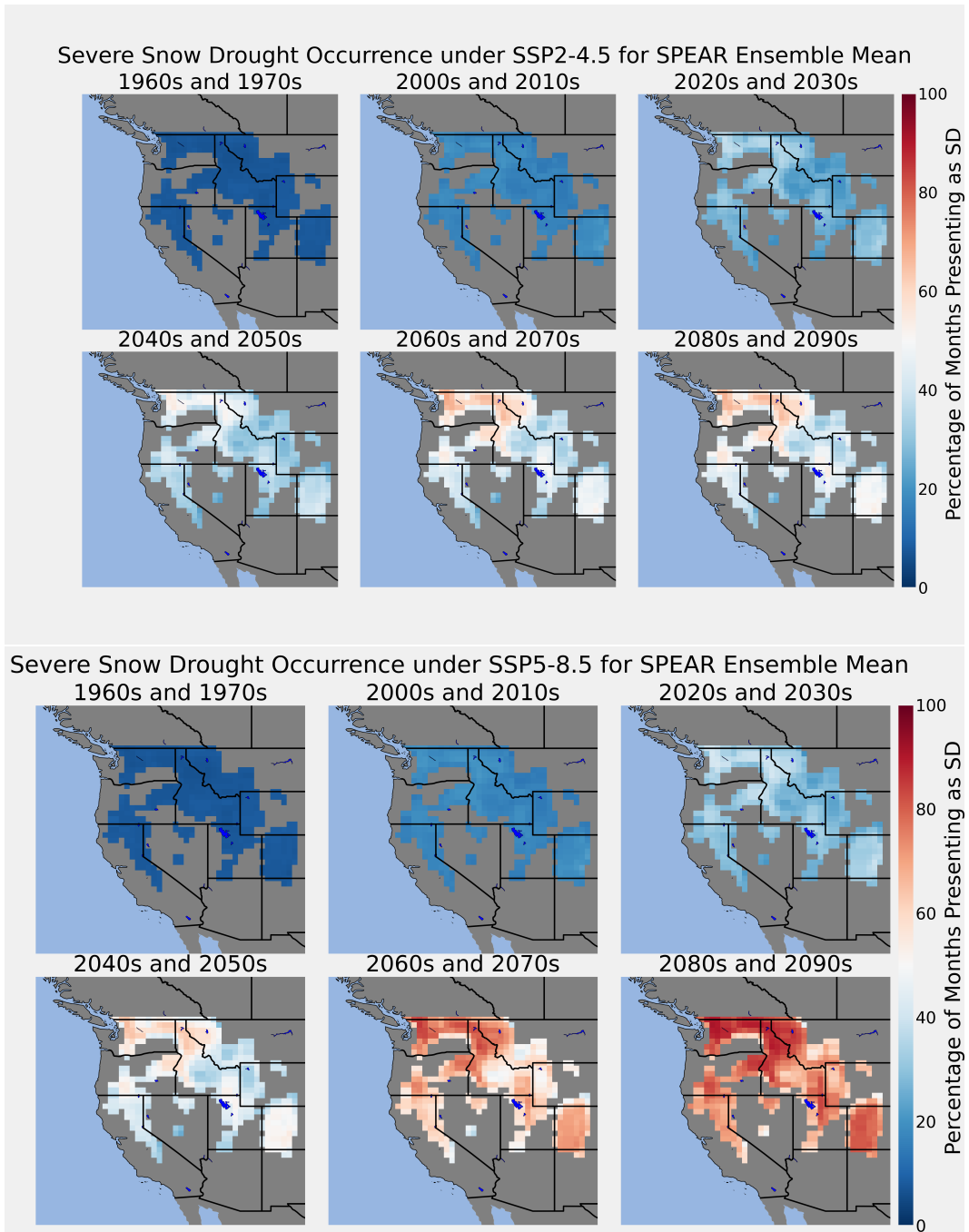


**Figure 4.** SPEAR snow drought changes highlighted from 1960-2100 under low (SSP2-4.5) and high (SSP5-8.5) emissions scenarios. The plots are masked to historically snowy regions which are colored by the percentage of winter months that the grid-cell experiences snow drought grouped every 2 decades. Historically snowy regions are characterized by having an average peak SWE of at least 20mm.

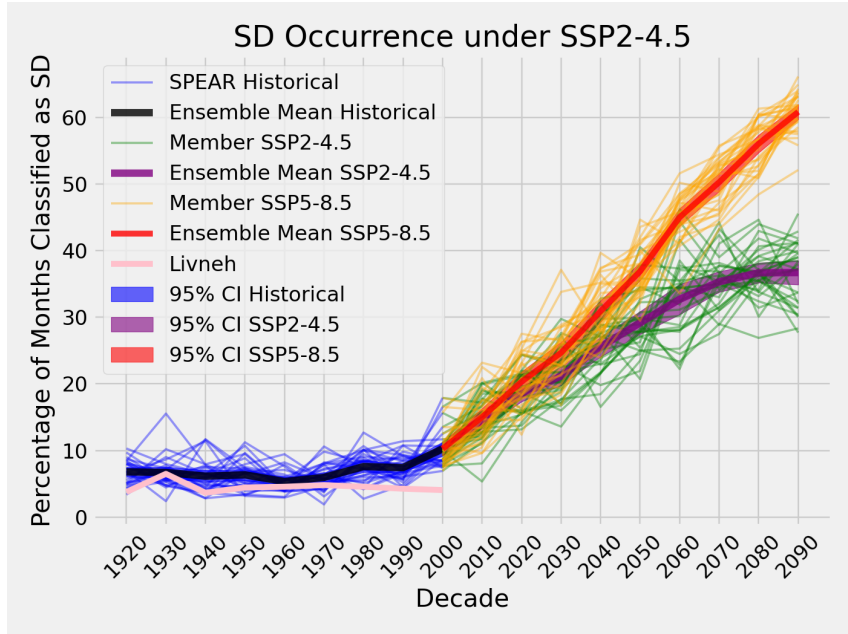


**Figure 5.** Decadal average of the number of SD months per grid cell. The green trend curves represent the ensemble mean averages for the historical and RCP 4.5 scenarios, while the orange curves depict the RCP 8.5 scenario. Ensemble mean and error is shaded darker.

itudes results in strong loss signals (Shrestha et al., 2021). We hypothesize that we are looking over a narrow enough range of latitudes that the latitude signal is overshadowed by regional variation, perhaps coming from elevation variability. Shrestha et al. (2021) looked at basins ranging from the Yukon to Columbia river basins that have average winter temperatures of  $-8^{\circ}\text{C}$  to  $+4^{\circ}\text{C}$ , finding that below  $-5^{\circ}\text{C}$  to  $-6^{\circ}\text{C}$  warming temperatures didn't reduce snowpack. Our HUC2 regions had mean winter temperatures in historically snowy regions ranging from  $-5.1^{\circ}\text{C}$  (UC) to  $0.3^{\circ}\text{C}$  (California), and so we expect that any warming will produce decreases in snowpack, and corresponding increases in D2+ SD occurrence.

While Figure 4 demonstrates the expected impacts of increasing greenhouse gases over the next century, as captured by the ensemble mean, it does not indicate how internal climate variability, as captured in the ensemble spread, may exacerbate or alleviate the radiatively forced changes. As regions must be prepared for conditions less favorable than an ensemble mean, the SPEAR large ensemble allows us to quantify the uncertainty of these ensemble mean changes that is attributable to internal variability. By aggregating across grid cells and then looking at changes for individual ensemble members as well as for the ensemble mean and 95%CI, we can visualize changes in the ensemble's snow drought through time (Figure 5).

Figure 5 shows the percentage of months by decade which experience D2+ SD in each of the SPEAR ensemble members. We find that members experience 5-12% D2+ SD frequency in the historical period, averaging 6.5% between 1920 and 2000. Under SSP5-8.5 this likelihood increases to over 35% snow drought frequency by 2050. Under SSP2-4.5, the same conditions are reached in 2070. We note the SSP5-8.5 curve is initially flat until 2000, where snow drought occurrence starts increasing and continues to grow unchecked; under SSP2-4.5 the curve has a second inflection point at 2070, where the increase in snow droughts flattens significantly.

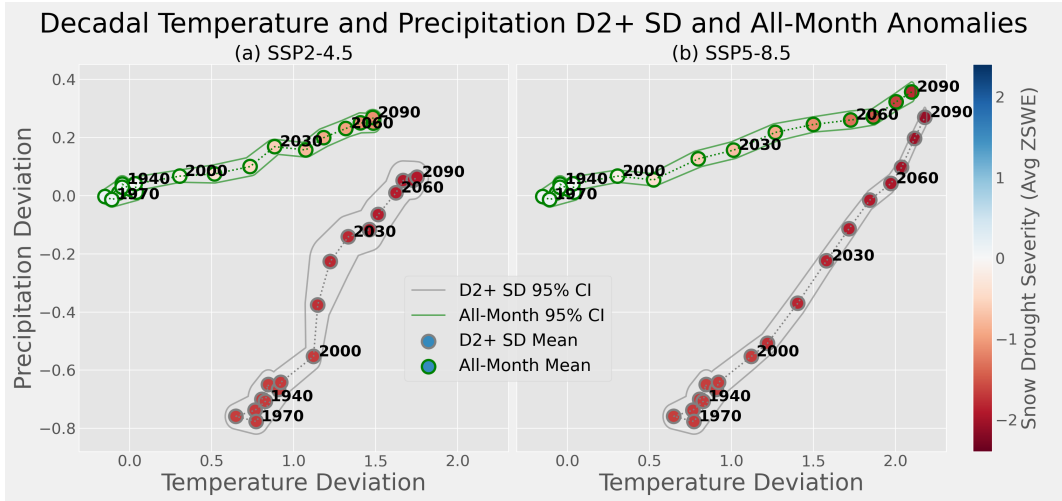


**Figure 6.** Temporal evolution of average temperature and precipitation anomalies with respect to the historical conditions (1921-2011). Each dot represents the average temperature and precipitation condition for historically snowy locations during winter (Oct-April) for a given decade either for all months and locations (outlined in green) or only for months classified as D2+ (outlined in gray). Each point is shaded by its average ZSWE score; thus because D2+ SD months are restricted to have a ZSWE of less than  $-1.3$ , these points average snow drought conditions are less than  $-1.3$ . Both all-month and D2+ SD-month points are surrounded by a contour which captures 95% of ensemble members. Panel (a) depicts these changes under SSP2-4.5 while (b) depicts changes under SSP5-8.5.

328

### 3.3 Temperature and Precipitation Controls on SWE

329  
330  
331  
332  
333

As changes in SWE are primarily driven by changes in temperature and precipitation climatology (McCrory et al., 2017; Harpold et al., 2017), we next examine changes in SWE in the phase space spanned by temperature and precipitation. By aggregating over the entire historically snowy Western United States, we can determine how temperature and precipitation anomalies are driving the dramatic increase of droughts.

334  
335  
336  
337  
338

In Figure 6, each dot represents the average temperature and precipitation anomaly by decade and is colored according to the average ZSWE score. By definition, the average all-month historical (1921-2011) temperature and precipitation mean is  $(0, 0)$ . However, by breaking the century down by decade we can see variation within the 20<sup>th</sup> century.

339  
340  
341  
342  
343  
344  
345  
346  
347  
348  
349  
350

As expected, points early in the historical period for the all month average cluster around zero temperature and precipitation deviation, and move as the underlying temperature and precipitation climatology shifts. In general we see very small changes in anomalies between decades before 2000. Beginning with the 2000s, the decadal averages for the all-month condition rapidly shift towards warmer and wetter conditions. For example, by 2050 under SSP5-8.5, the average temperature and precipitation are 1.50 and 0.25 standard deviations higher than the 20<sup>th</sup> century average, respectively. This corresponds to a dramatic warming and slight wetting across the WUS, and indicates that we expect the average month in 2050 to be warmer than 93% of months in the historical period for a given location. For SSP2-4.5, the values are 1.18 and 0.20, respectively, reflecting a still moderate increase in temperature and precipitation by mid-century, with the average month in 2050 being warmer than 88% of historical months.

To investigate how droughts specifically are changing, we average over just months which meet the D2+ criteria to see how the average drought month has changed (outlined in grey in Figure 6). We find that historical averages are both dry and warm with the average D2+ SD having a temperature and precipitation anomaly of 0.6 to 0.8 and -0.6 to -0.8, respectively, indicating historical snow droughts are primarily driven by a near equal combination of both warm and dry conditions. This corresponds to a drought month on-average being both warmer and drier than 75% of months.

However, by 2050 the average drought has become both warmer and *wetter*; under SSP5-8.5 the temperature deviation increases to 1.84 and the precipitation deviation increases to -0.015, meaning that it no longer takes any deviation from normal historical precipitation to produce a drought, and D2+ snow drought conditions are driven by the temperature average which is warmer than 97% of historical conditions. Under SSP2-4.5 the mean temperature and precipitation deviations are 1.51 and -0.065, respectively. By 2090, the average drought month has a temperature deviation of 2.18 and precipitation deviation of 0.27, very close to the all-month anomalies of 2.10 and 0.36 for temperature and precipitation respectively. Note that the average monthly temperature for both D2+ and all-month averages are in the 98th percentile of historical conditions, indicating not only that future winter conditions will on average be extremely warm, but that the difference between average conditions for all months and drought months alone has narrowed significantly. Examining the ZSWE scores for 2090 under SSP5-8.5 confirms the convergence, with the average all-month ZSWE being -1.79 and the average D2+ month having a ZSWE of -2.10. This corresponds to the all-month average falling in the D3, or extreme drought category, while the average drought is expected to be exceptional, or D4. Under SSP2-4.5, conditions do not become quite as extreme, with average all-month conditions by 2090 reaching 1.48 for temperature, 0.27 for precipitation, and -1.10 ZSWE. We note that although the gap to the D2+ condition narrows (1.75, 0.064, and -1.91 for T, P, and ZSWE), it is far less extreme than under SSP5-8.5; the average month is only given a D1 snow drought classification. The convergence of the all-month and D2+ temperature and precipitation anomalies, particularly under SSP5-8.5 emphasize that severe snow droughts will require increasingly smaller deviations from normal conditions to produce, underscoring that snow droughts will become the dominant regime in the WUS by the end of the 21<sup>st</sup> century.

### 3.4 Timeline for Snow Free Conditions

A no-snow regime, characterized by a 10-year moving average of April snowpack consistently below 10% of the historical April average, is potentially catastrophic as it indicates that summer water supply from snowpack will be severely limited. To understand when a no-snow regime is likely to affect an HUC2 region, we examine the distribution of transition times to no-snow across SPEAR's ensemble members. By varying the area threshold,  $\mathcal{A}$ , we can assess how quickly conditions are expected to deteriorate. Figure 7 shows the distribution of the transition to no snow regimes for 3 different area thresholds,  $\mathcal{A}$ : 50%, 75%, and 90%, for the historically snowy HUC2 regions. Note that by construction, an individual ensemble member's transition year always occurs later for higher  $\mathcal{A}$ . However the distributions themselves overlap, indicating large variability in the severity of conditions, especially later this century.

For  $\mathcal{A} = 0.5$ , we find that the West-Wide transition time, averaged across all regions is 2059 for SSP2-4.5 and 2040 for SSP5-8.5. Across regions however, transition times varied from as early as 2025 (CA) to 2088 (UC) for SSP2-4.5 and 2018 (CA) to 2056 (UC) for SSP5-8.5. Across all regions, the snow-free transition distribution is shifted later for SSP2-4.5 scenario when compared with SSP5-8.5, with more similar distributions between scenarios occurring in regions which experience a no-snow transition earlier, such as California. While a lower emission scenario improves the probability that the transition to a no-snow regime occurs later, internal climate variability could still result in periods of no snow much sooner than the ensemble mean predicts.

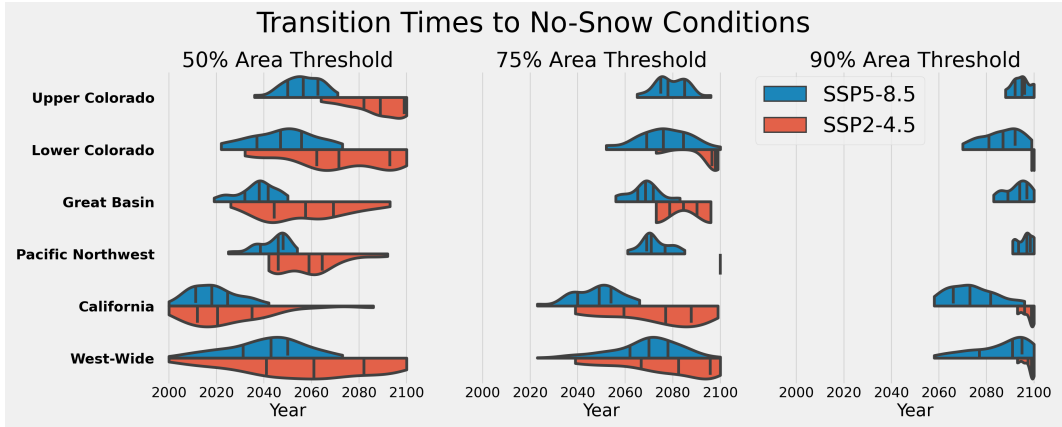


**Figure 7.** Distribution of SPEAR-simulated transition times to no snow regimes, or  $\mathcal{T}$ , by Western HUC2 region, split between SSP5-8.5 and SSP2-4.5 scenarios. The 3 subplots represent the different thresholds  $\mathcal{A}$ . Meeting a higher threshold corresponds with an increased proportion of the region experiencing perennial no-snow conditions, and implies more severe conditions. The vertical lines in the distributions represent the quantiles of the ensemble members that transition.

Another notable feature of Figure 7 is large range of transition times within each region of the 30-ensemble member transition times. We find that in some ensemble members, the earliest transition occurs over 15 years earlier than the median transition for many regions. For example, in the Lower Colorado region, the first ensemble member transitions to no-snow in 2069 while the mean transition time of the ensemble members isn't until 2086. Thus, while the LC is not likely to see these extreme conditions until the 2080s, according to SPEAR, their hydrological infrastructure, snow tourism economies, and fire response must be prepared significantly earlier to face these conditions. The shape of the ensemble spread under SSP2-4.5 differs significantly from the high emission scenario indicating a larger uncertainty in the onset of no-snow conditions. Under SSP2-4.5 the distribution of when the transition occurs in Figure 7 is more spread out and is centered later in comparison to the SSP5-8.5 distribution. This is consistent with our expectation that more rapid warming under SSP5-8.5 will accelerate the timeline associated with a transition to no-snow, the compressed timeline is simply a byproduct of this effect. In other words, temperature and precipitation changes are happening more slowly in SSP2-4.5 which leads to internal climate variability being a more important factor in determining no-snow transition times, as in SSP5-8.5 the accelerated radiative forcing is the dominant effect. As a result, many regions under SSP2-4.5 experience transition times that occur before ensemble members experiencing SSP5-8.5. For example, in the Pacific Northwest a quarter of the SSP2-4.5 realizations transitioned before the median ensemble member under SSP5-8.5. This suggests emission reductions, while likely to improve the odds that a no-snow transition occurs later in the century, do not a guarantee one. This is particularly true for regions where the transition is projected to occur earlier in the century, likely because the scenario forcing is much more similar.

To assess the probability that a region becomes snow free over the next century, we examine the fraction of ensemble members that transition to no-snow before 2100. We model the likelihood of the transition by the maximum likelihood estimator (MLE), or fraction of ensemble members that hit the transition threshold by 2100, and display these values in Table 8. By further splitting across the low and high emission scenarios, we can model how the risk also changes as a function of the radiative forcing scenario. In Table 8b, we see that under SSP5-8.5,  $\mathcal{A} = 0.75$  is guaranteed by 2100 across all re-

435 gions. The highest threshold,  $\mathcal{A} = 0.9$  is guaranteed only for California, while uncer-  
 436 tainty remains for the other 4 HUC2s. Conditions by 2100 are much less severe under  
 437 SSP2-4.5, with only  $\mathcal{A} = 0.5$  likely or certain for all regions, while for  $\mathcal{A} = 0.75$ , only  
 438 California is very likely to transition to a low snow regime; the other regions have low  
 439 probability of doing so. For  $\mathcal{A} = 0.9$  it is unlikely that any region will have transitioned  
 440 by 2100 under SSP2-4.5.

441 When we compare the order of how likely regions are to transition to no-snow con-  
 442 ditions under any scenario to the average mean historical temperature of historically snowy  
 443 areas, we find a striking similarity. Using SSP5-8.5 with a 90% area threshold as our ref-  
 444 erence column in Figure 8, and noting their mean winter temperatures we order from  
 445 least to most likely as UC (-5.1°C, 30%), PNW (-3.9°C, 53%), GB (-2.4°C, 70%), LC (-  
 446 0.7°C, 83%), and CA (0.3°C, 100%); the orderings are identical. This finding emphasizes  
 447 the role mean winter temperature plays in dictating a region’s no-snow transition prob-  
 448 ability. Like Shrestha et al. (2021) we find that warming any region with a winter av-  
 449 erage of  $> -5^\circ\text{C}$ , negatively impacts snowpack.

450 Strikingly, Table 8 indicates that under either SSP2-4.5 or SSP5-8.5 we expect at  
 451 least half of the historically snowy WUS to have less than 10% of its historical April snow-  
 452 pack by 2100. Both columns where  $\mathcal{A} = 50\%$  show  $> 80\%$  probability for all regions,  
 453 with the threshold guaranteed under SSP5-8.5. Strikingly, we also find that under SSP5-  
 454 8.5, 4 of the 5 Western watersheds are expected to cross our highest threshold of 90%  
 455 snow-free by 2100. Upper Colorado being the exception with only a 30% chance, likely  
 456 driven by it’s colder average winter temperatures. While these numbers are shocking,  
 457 it’s important to consider how snow-covered area and total snow volume differ. As snow-  
 458 pack declines have been dominated by losses at lower elevations that are closer to the  
 459 freezing point, we expect that the extreme loss of snow-covered area predicted by SPEAR  
 460 will overestimate the amount of total winter water storage lost, since the higher eleva-  
 461 tions typically store the most snowpack (Mote et al., 2005; Minder, 2009). Therefore we  
 462 expect the area-based no-snow transition to over-predict the hydrological impact of warm-  
 463 ing.

#### 464 4 Remarks

465 Widespread increases in D2+ snow droughts have already been observed in the his-  
 466 torical period, according to SPEAR, which estimates that across the WUS D2+ SD fre-  
 467 quency has increased by 43%, with an average 95% confidence interval of 22 to 65%. These  
 468 findings are slightly higher, although still consistent with, Huning and AghaKouchak (2020)  
 469 whose slightly different time period found a 28% increase in D2+ SD frequency for the  
 470 WUS over 1980–2018. SPEAR predicts even more dramatic changes heading into the 21<sup>st</sup>  
 471 century, classifying over 35% of winter months as snow droughts under RCP2-4.5 and  
 472 60% under RCP5-8.5 by 2100, compared with a normalized 9.6% across the historical  
 473 period. These changes were found to be primarily driven by increasing temperatures, which  
 474 on average exceeded the 93<sup>rd</sup> and 97<sup>th</sup> percentile (2 standard deviations) of historical  
 475 temperature records by 2100 under RCP2-4.5 and RCP4-8.5, respectively. We also found  
 476 that across all regions, the transition to a no-snow regime, where over 90% of the his-  
 477 torically snowy region had on average less than 10% of the April historical maximum,  
 478 was more likely than not in 4 out of the 5 HUC2s studied under RCP5-8.5, the UC re-  
 479 gion being the exception. Under RCP2-4.5, only the 50% threshold was exceedingly likely  
 480 for all regions, emphasizing the role that emissions this century will play in determin-  
 481 ing no-snow transition.

482 Similar to Shrestha et al. (2021), who found a strong correlation between decreas-  
 483 ing latitude and decreased snowpack, we find the probability of a no-snow transition is  
 484 much more likely for regions which have higher average winter temperatures. In partic-  
 485 ular, the Lower Colorado and California Regions, which are the most southern, had the  
 486 highest probabilities of reaching no-snow conditions across both emissions scenarios and

## Probability of No-Snow Transition by 2100

Region	SSP2-4.5			SSP5-8.5		
	50%	75%	90%	50%	75%	90%
Upper Colorado	83	0	0	100	97	30
Lower Colorado	87	23	7	100	100	83
Great Basin	100	7	0	100	100	70
Pacific Northwest	100	3	0	100	100	53
California	100	93	17	100	100	100

**Figure 8.** Probability of a snow free transition occurring before 2100 at the 3 thresholds  $\mathcal{A}$  based on the fraction of ensemble members who transition to a no-snow regime by 2100. We show the probabilities by area threshold, 50%, 75%, and 90%, across SSP2-4.5 and SSP5-8.5 for the historically snowy portions of each of the 5 Western HUC2 regions.

all area threshold values, and similarly had historical winter temperatures averaging near 0°C. The Pacific Northwest and Upper Colorado, the coldest regions on average, typically had the smallest transition probabilities.

While using a GCM allows us to examine multiple realizations of the climate to derive these probabilities, it is inherently limited by the model assumption constraints. In particular, the large resolution of a 1/2° global climate model is unable to resolve complex mountain topography and can result in significant warm biases which predicts less snow at elevation, as shown by Matiu and Hanzer (2022). We expect that this may make SPEAR snowpack estimates particularly sensitive to warming, and therefore likely to overestimate increases in snow drought. Another recent paper from Hoylman et al. (2022) asserts that using timescales longer than 30 years, as has been done in the vast majority of previous literature ((Svoboda et al., 2002)), as the baseline climatology can result in over-estimating the drought threat. Further work should be done to investigate the effect of the reference window on drought severity estimation.

Here, we've assessed changes in snow drought frequency, focusing on how the underlying climatology is expected to change, alongside modeling the distribution of expected no-snow transition times. This study has implications for Western hydrology, alongside snow tourism which is expected to see losses of 50% of ski season length by 2050 and 80% by 2090 (Wobus et al., 2017). One promising avenue for future research is to examine snow drought frequency changes over smaller regions, such as HUC4 regions to tease out which sub-regions are most vulnerable. This would also allow us to further examine latitude and elevation dependence. Also, estimating total SWE losses and melt timing across each region would allow us to better estimate the impacts of snow droughts on the West's hydrological system. The impacts of future snow droughts will be felt across the entire country, either directly from the hydrological or tourism resources that con-

512 sistent snowpack provides, or indirectly through loss of agricultural output from sum-  
 513 mer water shortages or drifting wildfire smoke and warrant further investigations.

514 **Acknowledgments**

515 Many thanks to Sarah Kapnick for helping to inspire this project. We would also like  
 516 to thank the NOAA Hollings Scholarship Program for funding this research.

517 **References**

- Barnett, T. P., Adam, J. C., & Lettenmaier, D. P. (2005, November). Potential  
 519 impacts of a warming climate on water availability in snow-dominated re-  
 520 gions. *Nature*, 438(7066), 303–309. Retrieved 2022-07-26, from <https://www.nature.com/articles/nature04141> (Number: 7066 Publisher: Nature  
 521 Publishing Group) doi: 10.1038/nature04141
- Delworth, T. L., Cooke, W. F., Adcroft, A., Bushuk, M., Chen, J.-H., Dunne,  
 523 K. A., ... Zhao, M. (2020). Spear: The next generation gfdl modeling  
 524 system for seasonal to multidecadal prediction and projection. *Journal of  
 525 Advances in Modeling Earth Systems*, 12(3), e2019MS001895. Retrieved  
 526 from <https://agupubs.onlinelibrary.wiley.com/doi/abs/10.1029/2019MS001895> (e2019MS001895 2019MS001895) doi: <https://doi.org/10.1029/2019MS001895>
- Deser, C., Lehner, F., Rodgers, K. B., Ault, T., Delworth, T. L., DiNezio, P. N., ...  
 530 Ting, M. (2020, April). Insights from earth system model initial-condition  
 531 large ensembles and future prospects. , 10(4), 277–286. Retrieved 2022-08-31,  
 532 from <https://www.nature.com/articles/s41558-020-0731-2> (Number: 4  
 533 Publisher: Nature Publishing Group) doi: 10.1038/s41558-020-0731-2
- Gergel, D. R., Nijssen, B., Abatzoglou, J. T., Lettenmaier, D. P., & Stumbaugh,  
 535 M. R. (2017). Effects of climate change on snowpack and fire potential in the  
 536 western USA. , 141(2), 287–299. Retrieved from <https://doi.org/10.1007/s10584-017-1899-y> doi: 10.1007/s10584-017-1899-y
- Harpold, A., Dettinger, M., & Rajagopal, S. (2017, 02). Defining snow drought and  
 539 why it matters. *Eos Transactions American Geophysical Union*. doi: 10.1029/  
 540 2017EO068775
- Hoyleman, Z. H., Bocinsky, R. K., & Jencso, K. G. (2022). Drought assessment has  
 542 been outpaced by climate change: empirical arguments for a paradigm shift. ,  
 543 13(1), 2715. Retrieved 2022-11-12, from <https://www.nature.com/articles/s41467-022-30316-5> (Number: 1 Publisher: Nature Publishing Group) doi:  
 544 10.1038/s41467-022-30316-5
- Huning, L. S., & AghaKouchak, A. (2020). Global snow drought hot spots and  
 547 characteristics. *Proceedings of the National Academy of Sciences*, 117(33),  
 548 19753–19759. Retrieved from <https://www.pnas.org/doi/abs/10.1073/pnas.1915921117> doi: 10.1073/pnas.1915921117
- Kim, R. S., Kumar, S., Vuyovich, C., Houser, P., Lundquist, J., Mudryk, L.,  
 551 ... Wang, S. (2021). Snow ensemble uncertainty project (seup): quanti-  
 552 tification of snow water equivalent uncertainty across north america via  
 553 ensemble land surface modeling. *The Cryosphere*, 15(2), 771–791. Re-  
 554 tried from <https://tc.copernicus.org/articles/15/771/2021/> doi:  
 555 10.5194/tc-15-771-2021
- Livneh, B., Rosenberg, E. A., Lin, C., Nijssen, B., Mishra, V., Andreadis, K. M.,  
 557 ... Lettenmaier, D. P. (2013). A long-term hydrologically based dataset  
 558 of land surface fluxes and states for the conterminous united states: Up-  
 559 date and extensions. *Journal of Climate*, 26(23), 9384 - 9392. Retrieved  
 560 from <https://journals.ametsoc.org/view/journals/clim/26/23/jcli-d-12-00508.1.xml> doi: 10.1175/JCLI-D-12-00508.1

- 563 Maher, N., Kay, J. E., & Capotondi, A. (2022). Modulation of ENSO teleconnec-  
 564 tions over north america by the pacific decadal oscillation. , 17(11), 114005.  
 565 Retrieved 2022-11-01, from <https://dx.doi.org/10.1088/1748-9326/ac9327>  
 566 (Publisher: IOP Publishing) doi: 10.1088/1748-9326/ac9327
- 567 Matiu, M., & Hanzer, F. (2022). Bias adjustment and downscaling of snow cover  
 568 fraction projections from regional climate models using remote sensing for the  
 569 european alps. *Hydrology and Earth System Sciences*, 26(12), 3037–3054. Re-  
 570 trieval from <https://hess.copernicus.org/articles/26/3037/2022/> doi:  
 571 10.5194/hess-26-3037-2022
- 572 McCrary, R. R., McGinnis, S., & Mearns, L. O. (2017). Evaluation of snow  
 573 water equivalent in narccap simulations, including measures of observa-  
 574 tional uncertainty. *Journal of Hydrometeorology*, 18(9), 2425 - 2452. Re-  
 575 trieval from [https://journals.ametsoc.org/view/journals/hydr/18/9/jhm-d-16-0264\\_1.xml](https://journals.ametsoc.org/view/journals/hydr/18/9/jhm-d-16-0264_1.xml) doi: 10.1175/JHM-D-16-0264.1
- 577 McCrary, R. R., Mearns, L. O., Hughes, M., Biner, S., & Bukovsky, M. S. (2022,  
 578 February). Projections of North American snow from NA-CORDEX and their  
 579 uncertainties, with a focus on model resolution. *Climatic Change*, 170(3), 1-25.  
 580 Retrieved from [https://ideas.repec.org/a/spr/climat/v170y2022i3d10.1007\\_s10584-021-03294-8.html](https://ideas.repec.org/a/spr/climat/v170y2022i3d10.1007_s10584-021-03294-8.html) doi: 10.1007/s10584-021-03294-
- 582 Minder, J. R. (2009). The sensitivity of mountain snowpack accumulation to climate  
 583 warming. *Journal of Climate*, 23, 2634 - 2650.
- 584 Mote, P. W., Hamlet, A. F., Clark, M. P., & Lettenmaier, D. P. (2005). Declining  
 585 mountain snowpack in western north america\*. *Bulletin of the American Mete-  
 586 orological Society*, 86(1), 39 - 50. Retrieved from <https://journals.ametsoc.org/view/journals/bams/86/1/bams-86-1-39.xml> doi: 10.1175/BAMS-86-1-39
- 587 Shrestha, R. R., Bonsal, B. R., Bonnyman, J. M., Cannon, A. J., & Najafi, M. R.  
 588 (2021). Heterogeneous snowpack response and snow drought occurrence across  
 589 river basins of northwestern north america under 1.0 °c to 4.0 °c global warm-  
 590 ing. *Climatic Change*, 164(3), 40.
- 591 Siirila-Woodburn, E. R., Rhoades, A. M., Hatchett, B. J., Huning, L. S., Szinai, J.,  
 592 Tague, C., ... Kaatz, L. (2021). A low-to-no snow future and its impacts  
 593 on water resources in the western united states. *Nature Reviews Earth &  
 594 Environment*, 2(11), 800–819. Retrieved from <https://doi.org/10.1038/s43017-021-00219-y> doi: 10.1038/s43017-021-00219-y
- 595 Svoboda, M., LeComte, D., Hayes, M., Heim, R., Gleason, K., Angel, J., ...  
 596 Stephens, S. (2002). The drought monitor. *Bulletin of the American Me-  
 597 teorological Society*, 83(8), 1181 - 1190. Retrieved from [https://journals.ametsoc.org/view/journals/bams/83/8/1520-0477-83\\_8\\_1181.xml](https://journals.ametsoc.org/view/journals/bams/83/8/1520-0477-83_8_1181.xml) doi:  
 598 10.1175/1520-0477-83.8.1181
- 599 Trujillo, E., Molotch, N. P., Goulden, M. L., Kelly, A. E., & Bales, R. C. (2012).  
 600 Elevation-dependent influence of snow accumulation on forest greening. ,  
 601 5(10), 705–709. Retrieved 2022-07-26, from <https://www.nature.com/articles/ngeo1571> (Number: 10 Publisher: Nature Publishing Group)  
 602 doi: 10.1038/ngeo1571
- 603 Wobus, C., Small, E. E., Hosterman, H., Mills, D., Stein, J., Rissing, M., ... Mar-  
 604 tinich, J. (2017). Projected climate change impacts on skiing and snowmobil-  
 605 ing: A case study of the united states. *Global Environmental Change*, 45, 1-14.  
 606 Retrieved from <https://www.sciencedirect.com/science/article/pii/S0959378016305556> doi: <https://doi.org/10.1016/j.gloenvcha.2017.04.006>
- 607 Wrzesien, M. L., Pavelsky, T. M., Durand, M. T., Dozier, J., & Lundquist, J. D.  
 608 (2019). Characterizing biases in mountain snow accumulation from global data  
 609 sets. *Water Resources Research*, 55(11), 9873-9891. Retrieved from <https://agupubs.onlinelibrary.wiley.com/doi/abs/10.1029/2019WR025350> doi:  
 610 <https://doi.org/10.1029/2019WR025350>